Supporting Information:

Enhanced sodium ion mobility in sodium tellurosilicates and crystal structures of Na_4SiTe_4 and $Na_{10}Si_2Te_9$ with isolated $[SiTe_4]^{4-}$ tetrahedra and isolated Te^{2-} anions

Franziska Kamm, Florian Pielnhofer,* Marc Schlosser, and Arno Pfitzner*

Institut für anorganische Chemie, Universität Regensburg, 93053 Regensburg, Germany

E-mail: florian.pielnhofer@ur.de; arno.pfitzner@ur.de

Contents

1 Na_4SiTe_4 **S-3**

2 $Na_{10}Si_2Te_9$ **S-4**

2.1 Structure Determination from Single Crystal X-ray Diffraction S-4

2.2 Structure Determination from Powder X-ray Diffraction S-11

3 $Na_6Si_2Te_6$ **S-15**

4 $Na_8Si_4Te_{10}$ **S-16**

5 Impedance Spectroscopy **S-17**

6 Calculation Details **S-18**

References **S-21**

1 Na_4SiTe_4

Table S1: Crystallographic data and details of structure determination of Na_4SiTe_4.

chemical formula	Na_4SiTe_4
powder color	yellow
T / K	293
crystal system	cubic
space group	$Pa\bar{3}$ (No. 205)
a / Å	13.0312(5)
V / Å^3	2212.84(2)
formula units Z	8
calculated density ρ_{calc} / g cm^{-3}	3.7847
diffractometer	STOE Stadi P, Debye-Scherrer geometry
radiation	MoKα ($\lambda = 0.709\,30$ Å)
measurement range $2\Theta_{\min}$ / $2\Theta_{\max}$	2.000° / 61.385°
2Θ step	0.015°
number of parameters / restraints	19 / 0
R_P, wR_P, R_{exp}	0.0422, 0.0567, 0.0326
goodness of fit	1.74
R_{gt}, wR_{gt} ($I > 3\sigma$)	0.0408, 0.0469
R_{all}, wR_{all}	0.0447, 0.0476
$\Delta\rho_{min}$, $\Delta\rho_{max}$ / e/Å^3	-1.36, 1.15

Table S2: Atomic coordinates and isotropic displacement parameters for Na_4SiTe_4.

atom	wyck. position	x	y	z	U_{eq} / Å^2
Na1	24d	0.7370(7)	0.2987(4)	0.4850(8)	0.048(2)
Na2	4a	0	0	0	0.04(1)
Na3	4b	1/2	1/2	1/2	0.04(1)
Si	8c	0.6372(4)	x	x	0.014(2)
Te1	24d	0.7490(1)	0.54036(5)	0.51226(7)	0.0260(3)
Te2	8c	0.7456(1)	x	x	0.0275(5)

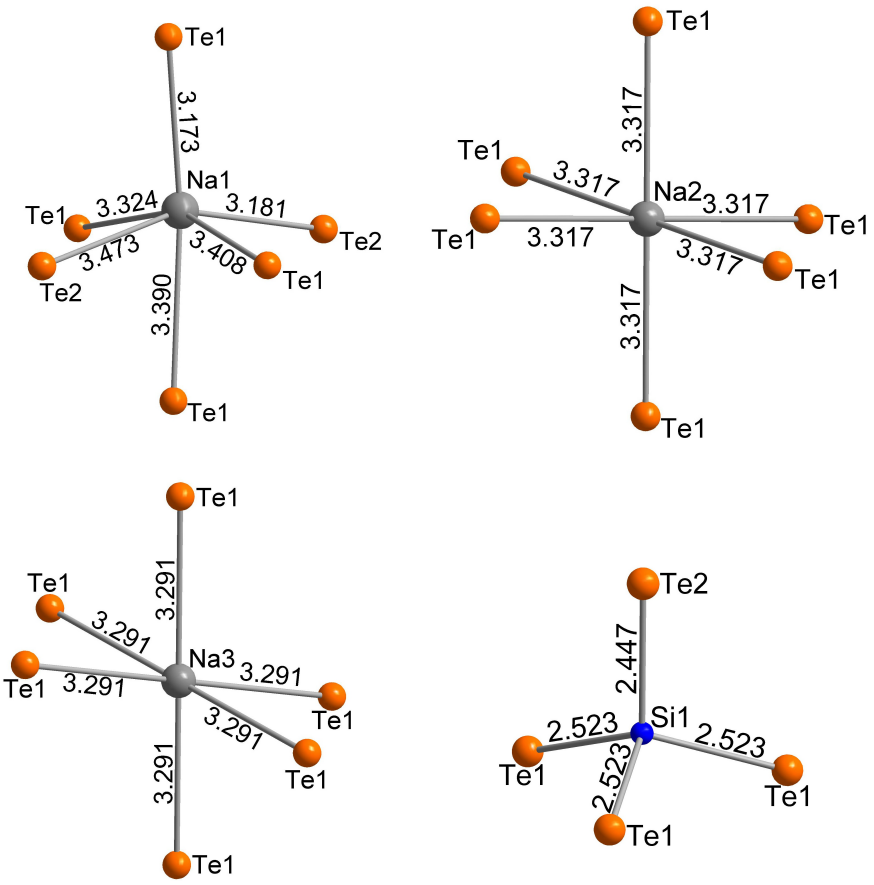

Figure S1: Coordination polyhedra of Na and Si in Na_4SiTe_4 with distances in Å.

2 $Na_{10}Si_2Te_9$

2.1 Structure Determination from Single Crystal X-ray Diffraction

Due to various problems during the structure determination of $Na_{10}Si_2Te_9$ several different crystals were measured at different temperatures and two different diffractometers (Rigaku SuperNova and Rigaku Synergy, DW systems) to exclude artifacts from bad crystal quality of individual crystals.

All determined structure models show rather high residual electron densities and R values are higher than expected. This can have various reasons, e.g. the assumed symmetry is

higher than the real symmetry or the measured data is affected by twinning which is leading to a wrong crystal structure.

The measured reflections can be indexed with a unit cell with orthorhombic metric. In all cases, more than 90 % of the reflections can be indexed. The measured diffraction pattern was also checked for twinning by the twin unit cell finding algorithm which is implement in *CrysAlisPro*[S1], but only small parts of unindexed reflections can be indexed to a second unit cell with the same lattice dimensions.

The orthorhombic metric, the statistics of $E^2 - 1$ and the observed absence conditions lead to the centrosymmetric space group *Pbcn* (No. 60). A structure model with both isolated $[SiTe_4]^{4-}$ tetrahedra and isolated Te^{2-} units with the composition $Na_{10}Si_2Te_9$ or $Na_{10}(SiTe_4)_2Te$, respectively was obtained from structure solution with direct methods. Though the structure model seems reasonable from a chemical point of view, the structure refinement was not entirely satisfactory. The resulting crystal structure exhibits high residual electron density around Te with distances less than 1 Å and converges with unexpected high R values. The crystallographic data and details of structure determination are shown in Table S3, exemplary for one of the analyzed crystals. Additionally, the structures exhibits some splitted sodium positions with a reduced occupancy of 50 % and short interatomic distances.

By refinement as inversion twin in space group $Pna2_1$ (No. 33), which is a subgroup of *Pbcn*, the suspicious sodium positions can be resolved to fully occupied positions with coordination spheres as expected. Also the R values dropped to more reasonable values. Besides that, the residual electron density remains higher as can be expected. The resulting crystallographic data and details of the structure determination are listed in Table S4. Note that all given data (refinement in *Pbcn* and $Pna2_1$) stems from the same measurement data.

To solve the problematic residual electron density (Figure S4), different further orthorhombic, monoclinic and triclinic space groups were tested. Also various twinning options did not lead to reasonable structure solutions.

Table S3: Crystallographic data and details of structure determination of $Na_{10}Si_2Te_9$ from single crystal X-ray diffraction in the centrosymmetric space group *Pbcn*.

chemical formula	$Na_{10}Si_2Te_9$
chemical formula weight / $g\,mol^{-1}$	1434.5
crystal color	red
T / K	100.1(4)
crystal system	orthorhombic
space group	*Pbcn* (No. 60)
a / Å	12.9530(7)
b / Å	14.8399(8)
c / Å	12.8235(7)
V / $Å^3$	2464.9(2)
formula units Z	4
calculated density ρ_{calc} / $g\,cm^{-3}$	3.8654
diffractometer	Rigaku XtaLAB Synergy R, DW system, HyPix-Arc 150
radiation	MoKα ($\lambda = 0.710\,73$ Å)
measurement method	ω - scans
measurement range $2\Theta_{min}$ / $2\Theta_{max}$	2.09° / 39.85°
index range *hkl*	-21 < h < 23, -26 < k < 24, -22 < l < 22
measured / independent reflections (R_{int})	66640 / 7335 (0.0332)
absorption coefficient $\mu_{MoK\alpha}$	$10.746\,mm^{-1}$
absorption correction	gaussian
transmission T_{min}, T_{max}	0.622 / 0.764
structure solution	*Superflip*
structure refinement	*Jana2006*
data / restraints / parameter	7335 / 0 / 105
goodness of fit	2.95
final R, wR [$I \geq 2\sigma(I)$]	4.60, 10.60
final R, wR [all data]	5.62, 10.71
$\Delta\rho_{min}$, $\Delta\rho_{max}$ / $e/Å^3$	-5.94, 9.93

Table S4: Crystallographic data and details of structure determination of $Na_{10}Si_2Te_9$ from single crystal X-ray diffraction in space group $Pna2_1$.

chemical formula	$Na_{10}Si_2Te_9$
chemical formula weight / $g\,mol^{-1}$	1434.5
crystal color	red
T / K	100.1(4)
crystal system	orthorhombic
space group	$Pna2_1$ (No. 33)
a / Å	12.8235(7)
b / Å	14.8398(8)
c / Å	12.9530(7)
V / Å^3	2464.9(2)
formula units Z	4
calculated density ρ_{calc} / $g\,cm^{-3}$	3.8654
diffractometer	Rigaku XtaLAB Synergy R, DW system, HyPix-Arc 150
radiation	MoKα ($\lambda = 0.710\,73$ Å)
measurement method	ω - scans
measurement range $2\Theta_{min}$ / $2\Theta_{max}$	2.09° / 39.85°
index range hkl	-23 < h < 21, -26 < k < 24, -22 < l < 22
measured / independent reflections (R_{int})	67682 / 11789 (0.0294)
absorption coefficient $\mu_{MoK\alpha}$	10.746 mm^{-1}
absorption correction	gaussian
transmission T_{min}, T_{max}	0.614 / 0.747
structure solution	*Superflip*
structure refinement	*Jana2006*
data / restraints / parameter	14472 / 0 / 190
goodness of fit	1.65
final R, wR [$I \geq 2\sigma(I)$]	3.23, 6.62
final R, wR [all data]	4.37, 6.79
$\Delta\rho_{min}$, $\Delta\rho_{max}$ / e/Å^3	-4.93, 8.06

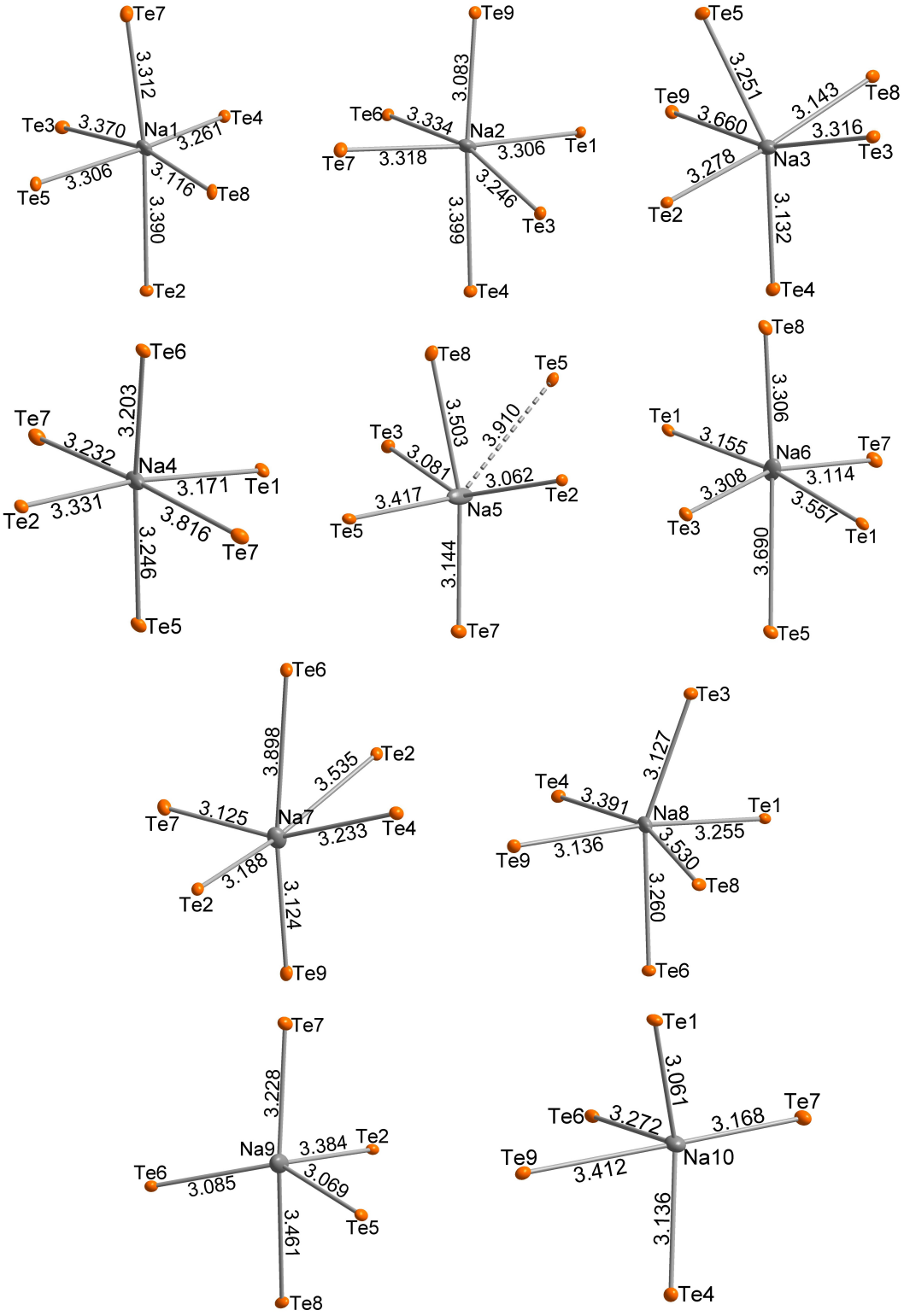

Figure S2: Coordination polyhedra of Na in $Na_{10}Si_2Te_9$ with distances in Å.

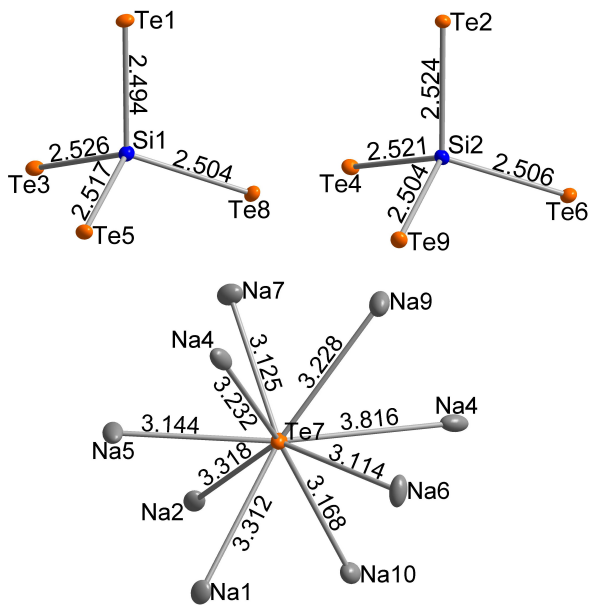

Figure S3: Coordination polyhedra of Si and Te9 in $Na_{10}Si_2Te_9$ with distances in Å.

Table S5: Atomic coordinates and isotropic displacement parameters for $Na_{10}Si_2Te_9$ from single crystal X-ray diffraction.

atom	wyck.	position	x	y	z	U_{eq} / Å^2
Na1		4a	0.1682(2)	0.4751(2)	-0.3719(3)	0.0167(8)
Na2		4a	-0.1654(2)	0.0285(2)	0.3684(3)	0.0179(8)
Na3		4a	0.0839(3)	0.6406(2)	-0.9438(3)	0.0197(9)
Na4		4a	-0.0242(2)	1.2537(2)	0.0043(2)	0.0206(6)
Na5		4a	0.0650(3)	0.5454(2)	-0.6053(3)	0.030(1)
Na6		4a	-0.2251(3)	-0.2388(2)	0.7128(2)	0.0234(8)
Na7		4a	0.2248(3)	0.7251(2)	-0.7294(3)	0.0219(7)
Na8		4a	-0.0903(2)	-0.1406(2)	0.9419(3)	0.0163(8)
Na9		4a	-0.2174(2)	-0.3650(2)	0.4565(2)	0.0254(7)
Na10		4a	-0.0591(2)	-0.0481(2)	0.5971(3)	0.0178(8)
Si1		4a	0.5071(2)	0.8490(1)	-0.2217(2)	0.0101(5)
Si2		4a	-0.5072(2)	-0.3510(1)	0.2242(1)	0.0089(5)
Te1		4a	0.5450(1)	0.6883(1)	-0.2636(1)	0.0093(1)
Te2		4a	-0.5476(1)	-0.1886(1)	0.2662(1)	0.0086(1)
Te3		4a	0.3678(1)	0.8470(1)	-0.0837(1)	0.0108(1)
Te4		4a	-0.3696(1)	-0.3462(1)	0.0854(1)	0.0099(1)
Te5		4a	0.4350(1)	0.9301(1)	-0.3767(1)	0.0101(1)
Te6		4a	-0.4327(1)	-0.4288(1)	0.3793(1)	0.0096(1)
Te7		4a	0.2511(1)	0.6518(1)	-0.5047(1)	0.0127(1)
Te8		4a	0.6665(1)	0.9289(1)	-0.1580(1)	0.0102(1)
Te9		4a	-0.6635(1)	-0.4334(1)	0.1568(1)	0.0102(1)

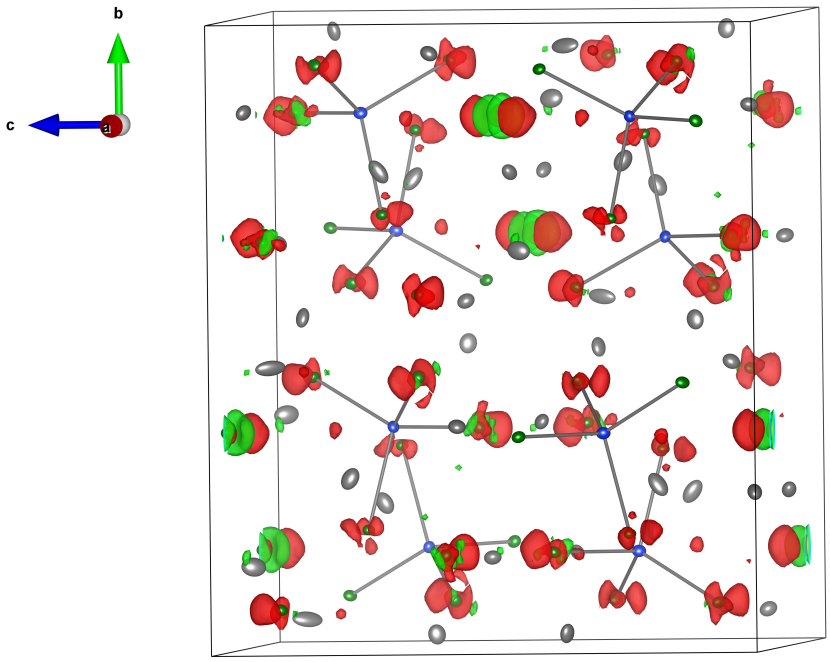

Figure S4: Difference Fourier map (F(obs)-F(calc)) with residual electron density near Te. For rendering a isosurface level of 1.2 was used.

Table S6: EDX analysis of crystalline $Na_{10}Si_2Te_9$. The analysis confirms the composition determined from X-ray diffraction experiments, which corresponds to 47.62 atom-% for Na, 9.52 atom-% for Si and 42.86 atom-% for Te.

element	mass norm. /%	atom-%	abs. error / %	rel. error / %
Na	15.73	46.68	0.96	6.36
Si	4.36	10.58	0.20	4.78
Te	79.92	42.73	2.28	2.96

2.2 Structure Determination from Powder X-ray Diffraction

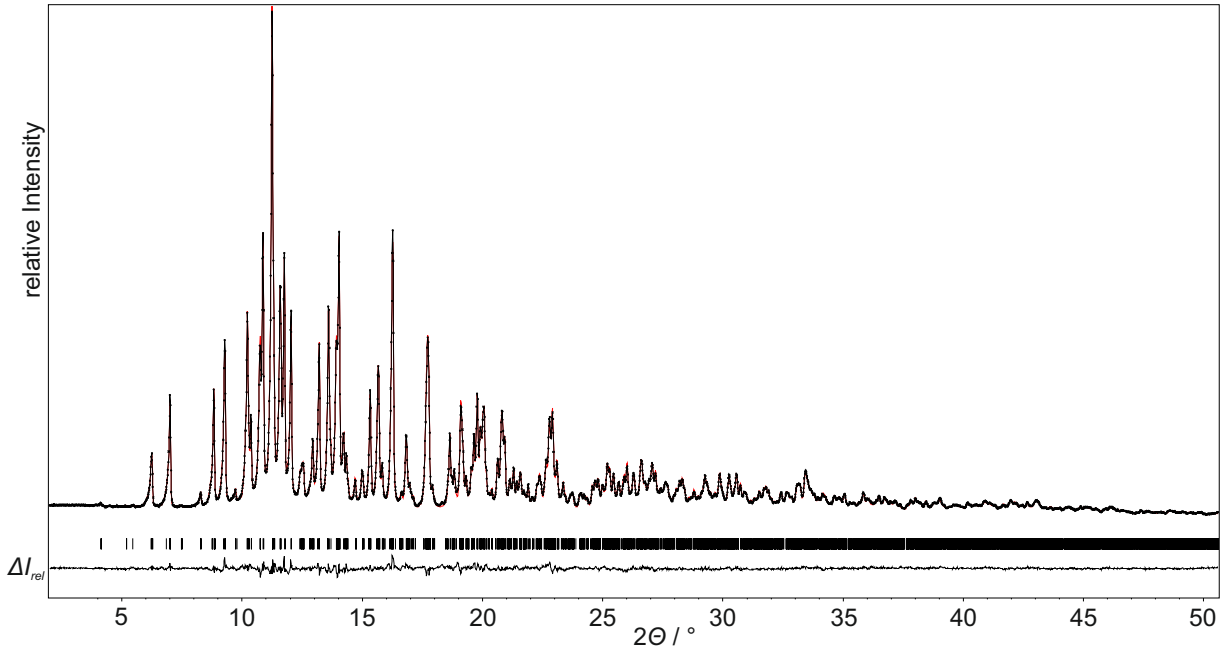

Figure S5: Powder diffraction pattern of $Na_{10}Si_2Te_9$ with difference plot from Rietveld refinement. The diffraction pattern was measured with MoKα_1 radiation ($\lambda = 0.7093\,\text{Å}$) at room temperature. For the structure refinement the structure model from single crystal diffraction was used.

Table S7: Crystallographic data and details of structure determination of $Na_{10}Si_2Te_9$ from powder X-ray diffraction.

chemical formula	$Na_{10}Si_2Te_9$
powder color	orange
T / K	293
crystal system	orthorhombic
space group	$Pna2_1$ (No. 33)
a / Å	12.9790(2)
b / Å	14.9308(2)
c / Å	13.0670(1)
V / Å^3	2532.21(5)
formula units Z	4
calculated density ρ_{calc} / g cm^{-3}	3.7627
diffractometer	STOE Stadi P, Debye-Scherrer geometry
radiation	MoKα ($\lambda = 0.7093$ Å)
measurement range $2\Theta_{min}$ / $2\Theta_{max}$	2.000° / 50.585°
2Θ step	0.015°
number of parameters / restraints / constraints	53 / 0 / 11
R_P, wR_P, R_{exp}	0.0211, 0.0272, 0.0139
goodness of fit	1.96
R_{gt}, wR_{gt} ($I > 3\sigma$)	0.0224, 0.0292
R_{all}, wR_{all}	0.0225, 0.0293
$\Delta\rho_{min}$, $\Delta\rho_{max}$ / e/Å^3	-0.61, 0.61

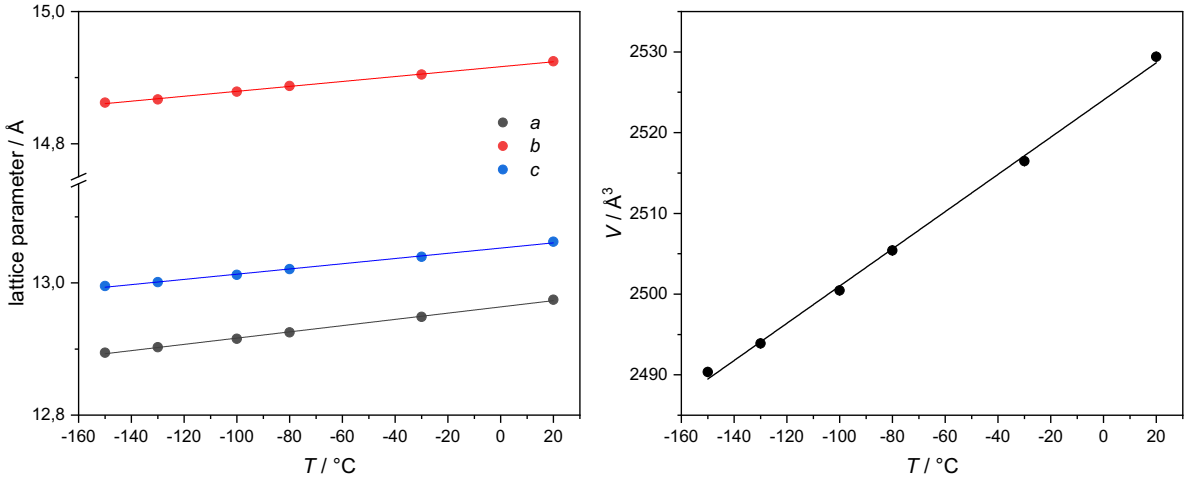

Figure S6: Lattice parameters of $Na_{10}Si_2Te_9$ at different temperatures. The parameters were determined via le Bail refinement from powder X-ray diffraction patterns. The linear course indicates no phase transition of $Na_{10}Si_2Te_9$ in the investigated temperature range (−150 °C to 20 °C).

Table S8: Atomic coordinates and isotropic displacement parameters for $Na_{10}Si_2Te_9$. Displacement parameters of Na and Si were restricted to be equal.

atom	wyck. position	x	y	z	U_{eq} / Å^2
Na1	4a	0.095(3)	0.647(2)	0.026(3)	0.063(2)
Na2	4a	0.255(3)	0.740(3)	0.377(3)	0.063(2)
Na3	4a	0.652(3)	0.031(2)	0.452(2)	0.063(2)
Na4	4a	0.417(2)	0.048(2)	0.212(2)	0.063(2)
Na5	4a	0.673(2)	0.518(2)	0.197(2)	0.063(2)
Na6	4a	0.454(2)	0.547(2)	0.500(2)	0.063(2)
Na7	4a	0.499(3)	0.236(3)	0.110(2)	0.063(2)
Na8	4a	0.215(2)	0.853(2)	0.556(2)	0.063(2)
Na9	4a	0.083(3)	0.130(3)	0.632(3)	0.063(2)
Na10	4a	0.226(3)	0.729(3)	0.821(3)	0.063(2)
Si1	4a	0.511(2)	0.349(1)	0.347(2)	0.009(3)
Si2	4a	0.505(2)	0.855(2)	0.2962(1)	0.009(3)
Te1	4a	0.5521(5)	0.1891(6)	0.3218(5)	0.031(2)
Te2	4a	0.5388(5)	0.6885(6)	0.3513(5)	0.032(2)
Te3	4a	0.6657(6)	0.4297(7)	0.4222(5)	0.045(3)
Te4	4a	0.4293(6)	0.4322(6)	0.2165(5)	0.040(3)
Te5	4a	0.6618(6)	0.9330(6)	0.2418(5)	0.029(2)
Te6	4a	0.4378(6)	0.9281(6)	0.4690(5)	0.030(2)
Te7	4a	0.3740(6)	0.3483(6)	0.5076(5)	0.037(3)
Te8	4a	0.3632(6)	0.8473(6)	0.1779(5)	0.030(2)
Te9	4a	0.250(1)	0.1530(2)	0.0903(9)	0.044(1)

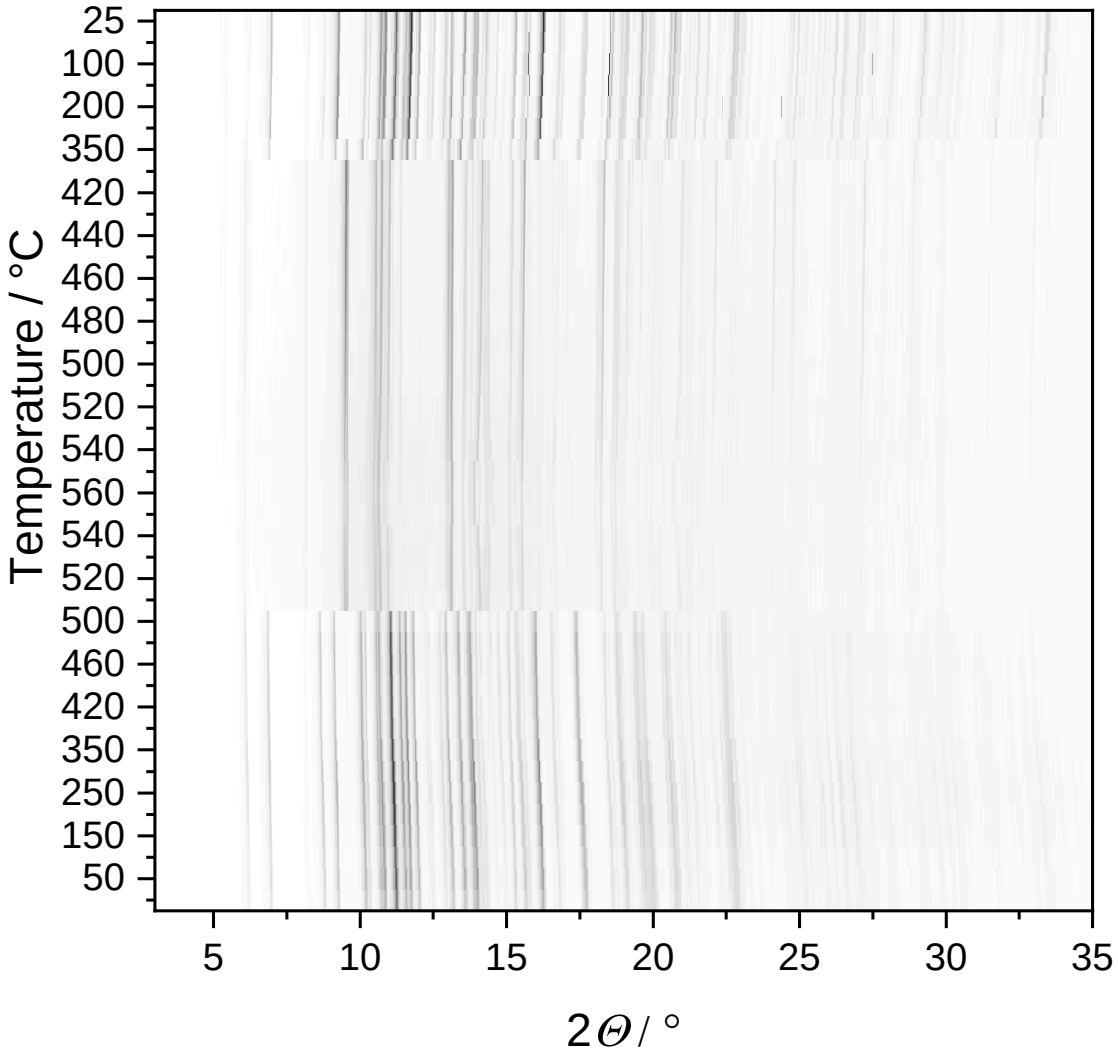

Figure S7: In situ high-temperature X-ray powder diffraction of $Na_{10}Si_2Te_9$ in the temperature range of 25 °C to 560 °C. $Na_{10}Si_2Te_9$ is present up to 500 °C. By further heating it decomposes and $Na_6Si_2Te_6$ and Na_2Te is formed. Upon cooling, the partial reformation of $Na_{10}Si_2Te_9$ can be observed.

3 $Na_6Si_2Te_6$

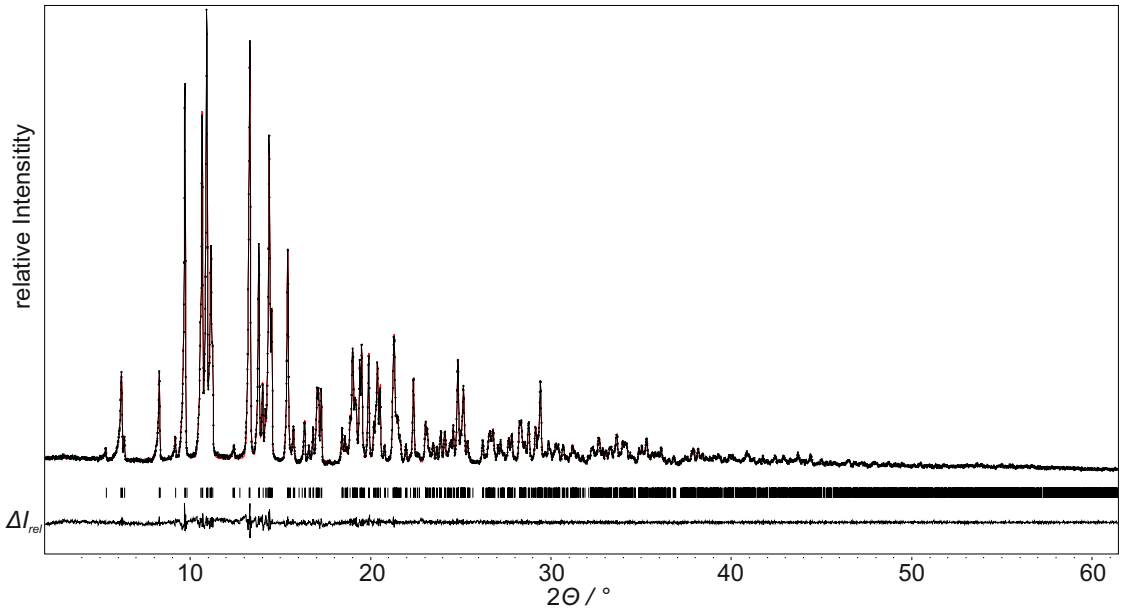

Figure S8: Refined powder diffraction pattern of $Na_6Si_2Te_6$ with difference plot, measured with MoKα_1 radiation ($\lambda = 0.7093\,$Å) at room temperature. For the le Bail refinement, the structure model of Eisenmann et al. was used.[S2]

Table S9: Unit cell parameters and R values from the refined powder diffraction pattern of $Na_6Si_2Te_6$.

	measured	literature[S2]
a / Å	8.7789(1)	8.786
b / Å	12.7801(2)	12.78
c / Å	8.8657(2)	8.864
β / °	119.749(2)	119.71
V / Å^3	863.60(3)	864.46
GOF	1.03	
R_P, wR_P, wR_{exp}	0.0320, 0.0447, 0.0436	

4 $Na_8Si_4Te_{10}$

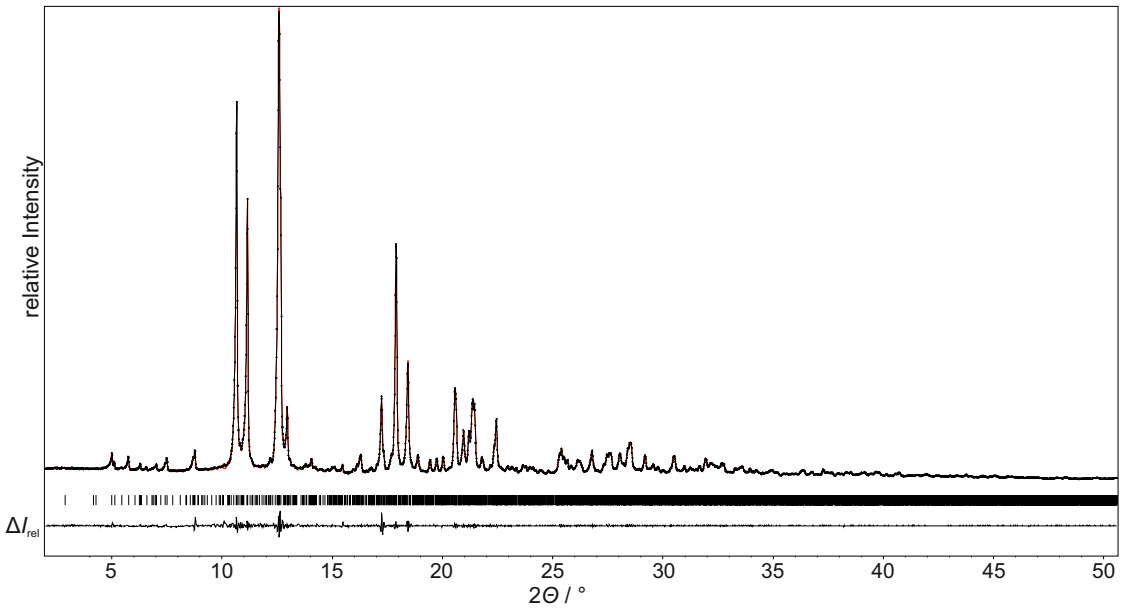

Figure S9: Refined powder diffraction pattern of $Na_8Si_4Te_{10}$ with difference plot, measured with MoKα_1 radiation ($\lambda = 0.7093$ Å) at room temperature. For the le Bail refinement, the structure model of Eisenmann et al. was used.[S3]

Table S10: Unit cell parameters and R values from the refined powder diffraction pattern of $Na_8Si_4Te_{10}$.

	measured	literature[S3]
a / Å	14.0843(2)	14.073
b / Å	12.8408(2)	12.842
c / Å	14.9389(3)	14.882
β / °	92.323(2)	92.22
V / Å^3	2699.54(9)	2687.54
GOF	1.73	
R_P, wR_P, wR_{exp}	0.0176, 0.0273, 0.0158	

5 Impedance Spectroscopy

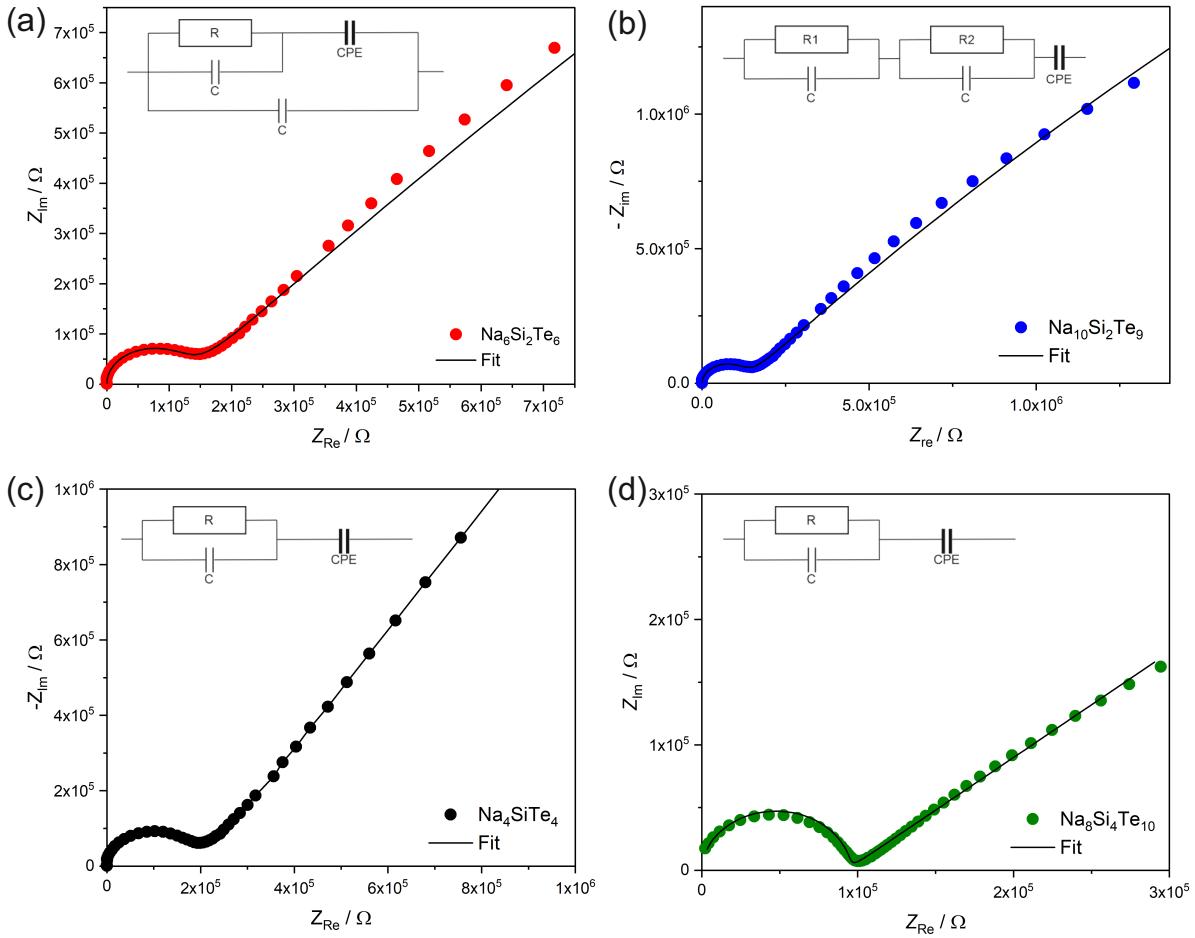

Figure S10: Nyquist plots including fit at 100 °C for $Na_6Si_2Te_6$ (a), $Na_{10}Si_2Te_9$ (b), Na_4SiTe_4 (c) and at 200 °C for $Na_8Si_4Te_{10}$ (d). Corresponding equivalent circuits for fitting of the Nyquist plots are also included.

6 Calculation Details

Basis sets were taken from the literature.[S4–S6] All basis sets are available in the basis set library at the Crystal homepage. The outer shells were adjusted so that the calculated energy was minimized. The basis sets used are as followed:

Table S11: Na basis set optimized for Na_4SiTe_4.

Na	exponent	contraction coefficient
$4sp$	0.1947	s: 1.0 p: 1.0
$3d$	0.1	1.0

Table S12: Si basis set optimized for Na_4SiTe_4.

Si	exponent	contraction coefficient
$6sp$	0.1527	s: 1.0 p: 1.0
$3d$	0.3335	1.0

Table S13: Te basis set optimized for Na_4SiTe_4.

Te	exponent	contraction coefficient
$5d$	0.2888	1.0

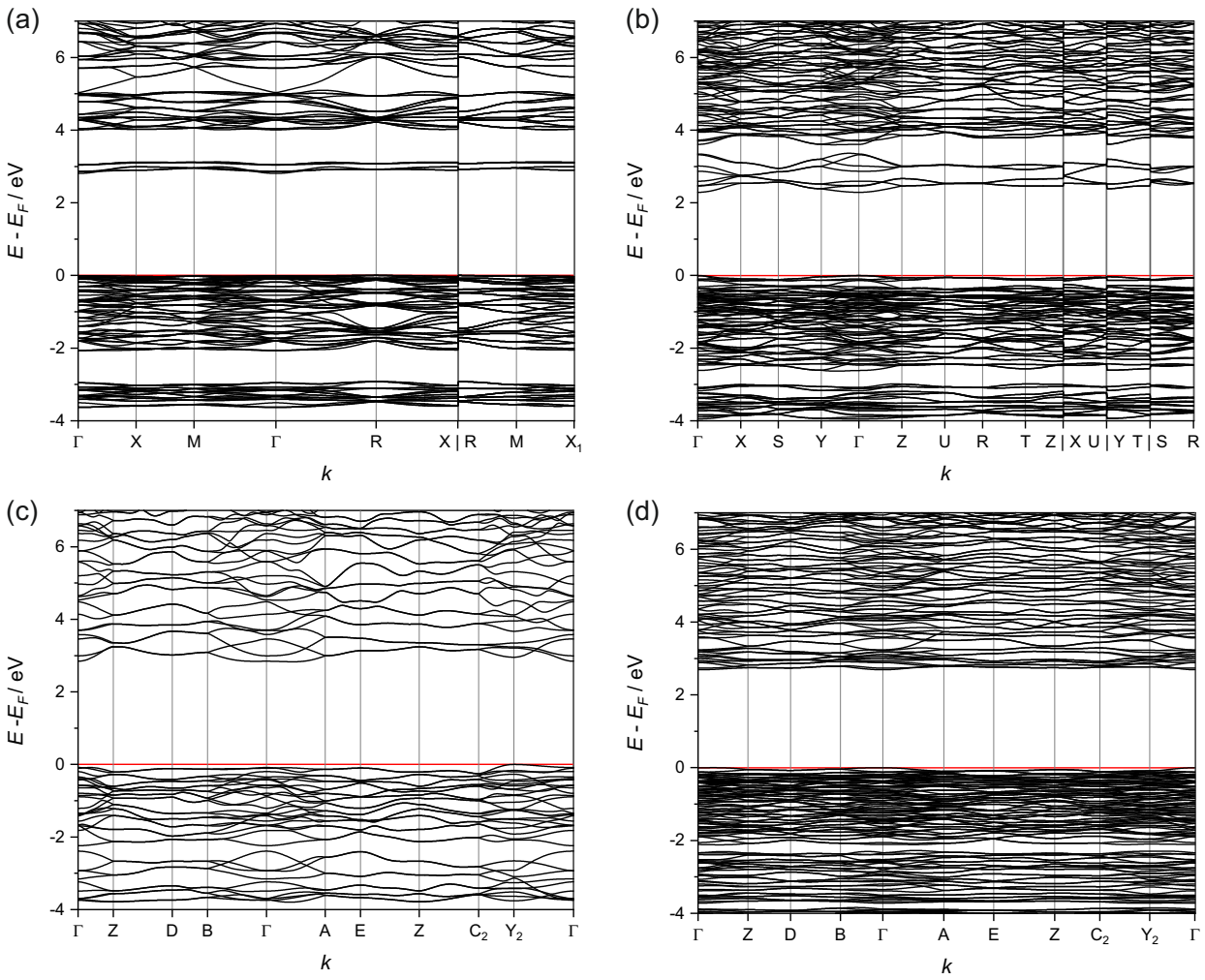

Figure S11: Calculated band structures of (a) Na_4SiTe_4, (b) $Na_{10}Si_2Te_9$, (c) $Na_6Si_2Te_6$ and (d) $Na_8Si_4Te_{10}$.

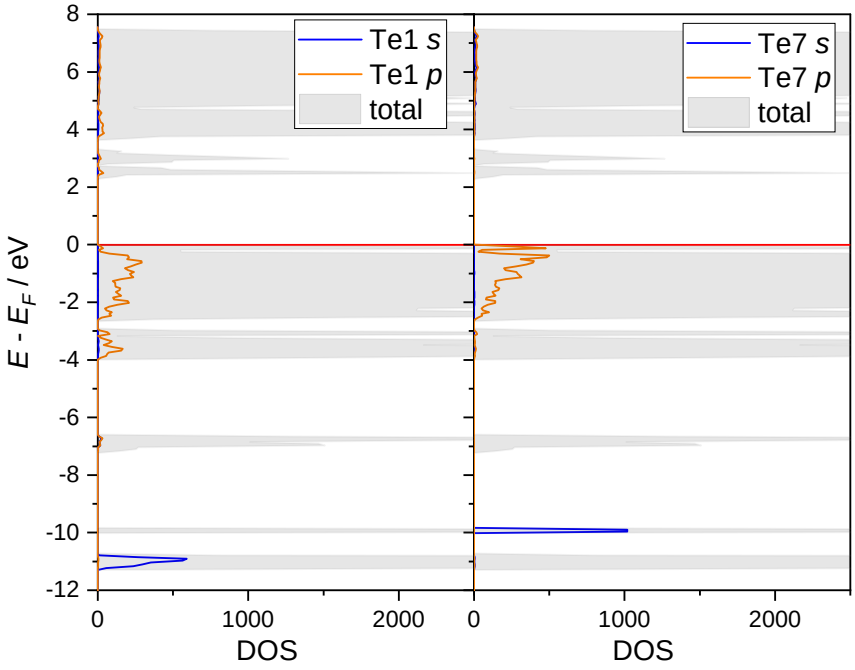

Figure S12: Orbital projected density of states for Te1 and Te7 in $Na_{10}Si_2Te_9$.

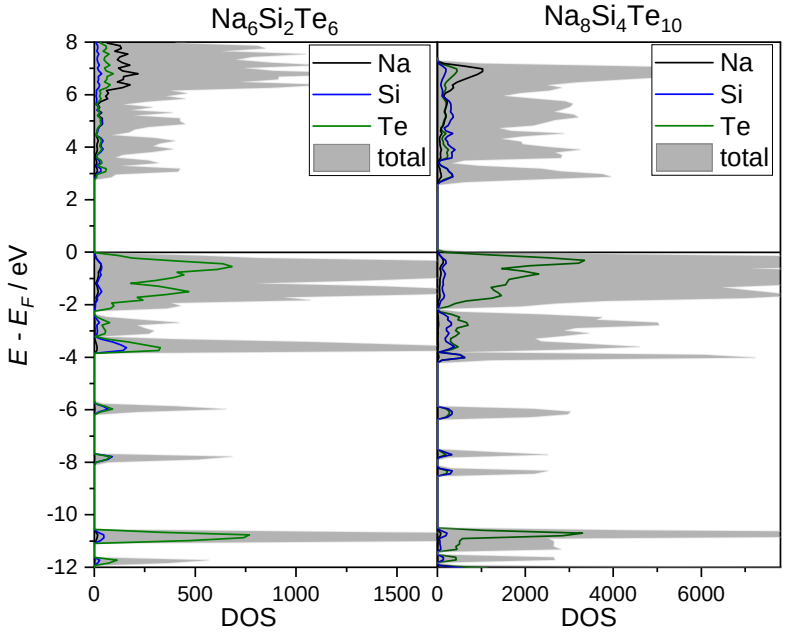

Figure S13: Electronic DOS of $Na_6Si_2Te_6$ and $Na_8Si_4Te_{10}$.

References

(S1) CrysAlisPro (V42). Rigaku Oxford Diffraction Ltd, 2019.

(S2) Eisenmann, B.; Schwerer, H.; Schäfer, H. $Na_6Si_2Te_6$ - ein neues Tellurohypodisilikat / $Na_6Si_2Te_6$ - A New Tellurohypodisilicate. *Z. Naturforsch. B* **1981**, *36*, 1538–1541.

(S3) Eisenmann, B.; Schwerer, H.; Schäfer, H. Neuartige Si4Te108- und Ge4Te108- - Anionen im Na8Si4Te10 bzw. Na8Ge4Te10. *Rev. chim. minér.* **1983**, *20*, 78–87.

(S4) Sophia, G.; Baranek, P.; Sarrazin, C.; Rerat, M.; Dovesi, R. `https://www.crystal.unito.it/Basis_Sets/sodium.html`, 2014; Accessed: 2023-03-06.

(S5) Porter, A. R.; Towler, M. D.; Needs, R. J. Muonium as a hydrogen analogue in silicon and germanium: Quantum effects and hyperfine parameters. *Phys. Rev. B* **1999**, *60*, 13534–13546.

(S6) Heyd, J.; Peralta, J. E.; Scuseria, G. E.; Martin, R. L. Energy band gaps and lattice parameters evaluated with the Heyd-Scuseria-Ernzerhof screened hybrid functional. *J. Chem. Phys.* **2005**, *123*, 174101.